Received: 1 March 2024 | Revised: 2 May 2024 | Accepted: 14 May 2024

DOI: 10.1002/aqc.4205

ARTICLE

WILEY

Growth and longevity of the endangered freshwater pearl mussel (*Margaritifera margaritifera*): Implications for conservation and management

Sabrina Nykänen | Jouni Taskinen | Mahsa Hajisafarali | Anna Kuparinen

Department of Biological and Environmental Science, University of Jyväskylä, Jyväskylä, Finland

Correspondence
Sabrina Nykänen, Department of Biological and Environmental Science, University of Jyväskylä, P.O. box 35 (YA), FI-40014 Jyväskylä, Finland.
Email: sabrina.s.nykanen@jyu.fi

Funding information
European Research Council, Grant/Award Number: 770884; Finnish Concordia Fund; Finnish Foundation for Nature Conservation; Kolarctic Cross Border Collaboration Programme, Grant/Award Number: KO1017; EU LIFE Programme, LIFE Revives, Grant/Award Number: LIFE20/NAT/FI/000611; Ellen and Artturi Nyyssönen Foundation; OLVI Foundation; Biological and Environmental Science Doctoral School of University of Jyväskylä

Abstract

Key life-history data, such as growth and age, are necessary to effectively manage and conserve threatened freshwater mussel species. Traditionally growth and age studies require large yet destructive sample sizes covering all age classes. Such methods pose a risk to populations of conservation concern, and therefore, alternative methods that need only limited sample sizes are necessitated to prevent further threats to such populations. We applied retrospective shell growth at age reconstructions to 98 critically endangered freshwater pearl mussel (FPM) individuals from 34 populations across Finland and Sweden, enabling the use of extremely small sample sizes ($n = 1$–6 per population). We compared the performance of six different growth models with the reconstructed size-at-age data across FPM juvenile (<20 years old) and adult life stages. The growth reconstruction model showed reasonable skill in reconstructing FPM growth patterns. The von Bertalanffy model showed to be a good general descriptor of growth for FPM, but it systematically underestimated the asymptotic size. The power law model was the most accurate in estimating juvenile growth (lowest deviances from the size-at-age data). FPM showed great variability in longevity ($A_{max} = 54$–254 years) and growth constant k (0.018–0.057 year^{-1}). Our results show that reasonable estimates of growth can be attained even when sample sizes are extremely limited. The results can be further applied to gain knowledge on the population's age structure, size at maturation, and recovery potential. The methodology is applicable to other freshwater mussel species of conservation concern.

KEYWORDS

age determination, back calculation, Bivalvia, endangered species, growth models, growth reconstruction, Unionida

1 | INTRODUCTION

Freshwater mussels (Unionida) are a diverse and widespread group of organisms, which have numerous important functional roles in freshwater ecosystems (Atkinson & Vaughn, 2014; DuBose et al., 2019). As filter feeders that often dominate benthic biomass, freshwater mussels contribute particularly to water purification, benthic-pelagic coupling, bioturbation and nutrient cycling (Howard &

Cuffey, 2006; Strayer, 2014; Vaughn, 2018; Vaughn & Hakenkamp, 2001). However, due to anthropogenic activities, endemic freshwater mussels are highly imperilled and declining at some of the highest known rates worldwide, which has made them the focus of extensive conservation efforts (Geist et al., 2023; Lopes-Lima et al., 2017; Régnier et al., 2009; Strayer et al., 2004).

Freshwater mussel species differ from each other especially in allocation to growth, which is reflected in great variation in growth parameters and longevity (Haag & Rypel, 2011). Somatic growth plays a key role in population dynamics and conservation biology because it strongly influences other central life-history traits, such as age at maturity, fecundity, survival and longevity (Charnov, 1993; Haag, 2013; Roff, 1992; Stearns, 1992). Understanding the characteristic of somatic growth is therefore fundamental in development of effective population conservation and management strategies for exploited or imperilled organisms (e.g., Ricker, 1975). While phylogeny constrains to some extent the life-history traits in freshwater mussels, within species growth and longevity show considerable plasticity in response to local environmental conditions, such as temperature and hydrochemistry (Bauer, 1992; Haag & Rypel, 2011; Jokela & Mutikainen, 1995). Because of the substantial plasticity in growth and longevity, generalizations of existing growth and age data from other species or even populations of the same species should be avoided as they can lead to wrong conclusions on the dynamics of a population of interest and ineffective or even harmful management and conservation strategies.

Several mathematical functions have previously been used for studying the age-dependent growth patterns in freshwater mussels, but von Bertalanffy's (1938) growth function remains the most applied in literature (e.g., Haag & Rypel, 2011). Despite its wide use in growth studies for organisms expressing indeterminate growth (i.e., continuously through life), the von Bertalanffy growth function does not always perform well with growth in the youngest age classes (Gamito, 1998; Hastie et al., 2000; Miguel et al., 2004). Thus, to characterize adequately the growth of a given species or individual, it may be necessary to compare the performance of alternative models to von Bertalanffy. Further, traditionally growth models require size-at-age data collected from multiple individuals of different sizes and ages from the same population to cover the growth trajectory from juvenile to adult because the models are highly dependent on having observations for all the age classes (Haag, 2009; Kritzer et al., 2001; Pardo et al., 2013). In the case of imperilled species, collection of live samples for growth and age studies is however often restricted because of the risk of destructive sampling. Helama and Valovirta (2008) addressed this problem by creating a model with which is possible to reconstruct the growth trajectories of freshwater mussels with internal annual growth increments determined in age studies. The model helps limiting destructive sampling in endangered populations in several ways. Firstly, it allows growth history reconstruction without mussel juveniles, which may be limited in unviable freshwater mussel populations. Second, reconstructing shell growth for size-at-age estimates makes it possible to conduct growth analyses without significantly reducing the number of reproductive individuals in the population as it reduces the number of live samples needed for growth analysis. Third, the model can also be applied to museum shell collections and to already existing growth data obtained from literature, making it an ethical technique of studying growth in endangered freshwater mussel species. In addition, the Helama and Valovirta (2008) model makes possible to produce growth trajectories and parameters at individual level, thus study the variation in growth within the populations of interest.

Among Unionida, freshwater pearl mussel (FPM) *Margaritifera margaritifera* (Linnaeus, 1758) is a slow-growing and extremely long-lived species (Dunca et al., 2011; Haag & Rypel, 2011) that inhabits oligotrophic streams and rivers in the Holarctic region (Geist, 2010; Young et al., 2001). FPM is assessed as critically endangered and under threat of worldwide extinction without prompt conservation actions (Cuttelod et al., 2011; Lopes-Lima et al., 2017). Although the threats to FPM are manyfold (e.g., habitat deterioration, decline of host fish populations), low recruitment due to high juvenile mortality is considered the biggest factor affecting the decline of FPM populations (Geist, 2010; Österling et al., 2008). Studies on the age-dependent growth patterns of FPM in different populations can provide substantial information for effective conservation of the species. For example, growth patterns can be used to transform existing size distributions, measured as part of viability studies, into more accurate population specific age distributions. From conservation perspective, it is important to know the age structure of populations of interest as it highly influences the population's growth and recovery potential: different age groups have different reproductive capabilities and rates of mortality (Charnov, 1993; Roff, 1992; Stearns, 1992). In addition, it is important to study the size of juveniles in different populations, as the proportion of juvenile mussels (less than 20 and 50 mm in length) is one of the main criteria in judging viability of FPM populations, but currently the criteria does not take into account population specific size differences at juvenile age (Oulasvirta et al., 2017). Given that FPM is critically endangered and that sample collection for age and growth studies is limited, it represents an ideal candidate for the appliance of the previously presented shell growth reconstruction model for conservation purposes. The present study not only contributes to the conservation of one highly vulnerable species but also, more generally, demonstrates research practices that avoid destructive sampling while still gathering substantial life-history trait information — methodology that can be readily applied to other freshwater mussel species of conservation concern.

In the present study we determined ages of 108 individuals and reconstructed the growth patterns of 98 individuals from 34 FPM populations across Finland and Sweden by applying the previously validated model by Helama and Valovirta (2008). We then compared the performance of several growth models in both juvenile and adult life stage. Therefore, the main aims of this study were to (1) reconstruct the growth patterns of mussel individuals using age determination data, (2) estimate the growth parameters and longevity of target populations, (3) investigate the among and within population variation in these parameters, (4) compare the performance of different growth models, and (5) find a suitable model for estimating the size of juveniles.

2 | MATERIALS AND METHODS

2.1 | Study area and sampling

In total, 29 rivers in northern Finland and 5 rivers in northern Sweden with resident FPM populations were sampled in the summer between 2019 and 2021 (June–September, Figure S1) as part of the European Neighbourhood Instrument Cross-Border Cooperation (ENI CBC) Kolarctic project 'SALMUS'. Because of the endangered status of FPM, the collection of living individuals was performed with special permissions granted by the regional Centres for Economic Development, Transport and the Environment of Kainuu (KAIELY/296/2019 and 357/2019), North Ostrobothnia (POPELY/1276/2019 and 1490/2019) and Lapland (LAPELY/1929/2019 and 2252/2019) in Finland; and by the County Administrative Board of Norrbotten (623-7408-2020) in Sweden. Only rivers with population

TABLE 1 Observed maximum shell length (L_{max}, mm), shell height (H_{max}, mm) and age (A_{max}, years) for 29 Finnish and five Swedish freshwater pearl mussel (*Margaritifera margaritifera*) populations.

Country	Basin	Catchment	River	*n*	L_{max}, mm	H_{max}, mm	A_{max}, years
Finland	Barents Sea	River Teno	Lovttajohka	3	120	57	254
	Barents Sea	River Tulomajoki	Hanhioja	3	94	44	58
	Barents Sea	River Tulomajoki	Kivijoki	3	98	54	134
	Barents Sea	River Tulomajoki	Kolmosjoki	3	122	58	98
	Barents Sea	River Tulomajoki	Lutto	3 (+3)	135	65	215
	Barents Sea	River Tulomajoki	Nohkimaoja	3	102	45[a]	120
	Barents Sea	River Tulomajoki	Suomujoki	3	127	48[a]	134
	Barents Sea	River Tulomajoki	Torkojoki	3	110	46[a]	113
	Barents Sea	River Tulomajoki	Urakkajärvenoja	2 (+2)	111	46[a]	110
	Barents Sea	River Tulomajoki	Vuoksioja	1	95	41[a]	54
	Baltic Sea	River Kemijoki	Ahvenoja	3	120	54	93
	Baltic Sea	River Kemijoki	Haukijoki	3	107	50	76
	Baltic Sea	River Kemijoki	Satsijoki	3	102	45	97
	Baltic Sea	River Kemijoki	Saukko-oja	3	101	43	107
	Baltic Sea	River Kemijoki	Siikajoki	3	115	52	77
	White Sea	River Koutajoki	Juumajoki	3	120	55	127
	White Sea	River Koutajoki	Merenoja	3	140	64	150
	White Sea	River Koutajoki	Myllyoja	3	103	48	100
	White Sea	River Koutajoki	Porontimajoki	3	92	44	81
	White Sea	River Koutajoki	Salmipuro	3	116	53	76
	White Sea	River Kem (Viena)	Juomajoki	3	117	58	100
	Baltic Sea	River Iijoki	Haukioja	3	110	50	80
	Baltic Sea	River Iijoki	Livojoki	2	102	52	110
	Baltic Sea	River Iijoki	Lohijoki	3	138	65	104
	Baltic Sea	River Iijoki	Nuottipuro	3	104	48	100
	Baltic Sea	River Oulujoki	Humalajoki	3	108	55	93
	Baltic Sea	River Oulujoki	Mutajoki	3	83	41	88
	Baltic Sea	River Oulujoki	Nuottijoki	3 (+5)	113	56	109
	Baltic Sea	River Oulujoki	Varisjoki	3	117	52	125
Sweden	Baltic Sea	River Lule	Souksaurebäcken	3	97	46	75
	Baltic Sea	River Lule	Varjekbäcken	3	117	53	94
	Baltic Sea	River Pite	Bölsmanån	3	131	59	92
	Baltic Sea	River Pite	Ljusträskbäcken	3	115	52	61
	Baltic Sea	River Pite	Tvättstugubäcken	3	91	42	72

Note: Number of age-determined living individuals is indicated by *n* and number of empty shells collected is in brackets. Total number of individuals retained for age determined was 108, of which in total 98 individuals were ≥50 years old and used in the shell reconstruction model.

[a]Measured in laboratory from the shell cross-section produced for age determination.

size ≥1000 individuals were included in the present study. Within each river, in total 30 mussel individuals were sampled randomly from a representative location by snorkelling. All the mussels were measured with a vernier calliper for length and height. From the 30 individuals, three largest were retained (for exceptions, see Table 1) for age determination, making a total of 108 individuals. The rest of the random sample was returned alive to their collection sites. The retained individuals were immediately stored in ice and transported alive to the laboratory at the Department of Biological and Environmental Science, University of Jyväskylä, Finland. The mussel individuals were originally retained to determine their age from shells, but in addition, their tissues were individually stored accordingly for possible further analyses — such as DNA, stable isotopes, fatty acids, metals, parasites and morphology — the results of which are not presented here.

2.2 | Age determination and annual growth increments

Age determination and measurement of the internal annual shell growth increments were performed in the Department of Palaeozoology, Swedish Museum of Natural History in Stockholm. Following the methods described by Dunca and Mutvei (2001), thin cross-sections were produced from one shell valve per mussel individual by cutting them perpendicularly to the annual growth rings (i.e., from the umbo to the marginal border). After being grinded and polished, the shell cross-sections were etched in Mutvei's solution for 30 min at 40°C to improve the visibility of the winter lines and the precision of age estimations (Schöne et al., 2005). The shell cross-sections were photographed with a reflective light microscope equipped with Carl Zeiss AxioCam camera. Using photographic enlargements, the internal annual growth increments were counted from the ventral margin to the beginning of the eroded part of the shell and measured to the nearest 1 μm as the minimum vertical distance between two winter lines in the prismatic (i.e., outer) shell layer, close to the nacreous layer's boundary line. The age of the eroded part in each shell was estimated with growth curves representing high, normal and low shell growth (Dunca et al., 2011). The age of the mussel was estimated by summing the number of the counted growth increments and age of the corroded part of the shell. For all populations, maximum observed age (A_{max}, years), length (L_{max}, mm) and height (H_{max}, mm) were obtained.

2.3 | Reconstructing shell growth for height-at-age estimates

We used a model developed by Helama and Valovirta (2008) to reconstruct the shell height growth history of each mussel individual throughout their life span. The model uses the observed annual shell growth increments measured from the shell cross-section to translate the convexly proceeding shell height growth (according to valve shape) into height-at-age estimates along the commissural plane — the direction from which the shell height is typically measured with venier callipers (see Figure 2 in Helama & Valovirta, 2008). In Helama and Valovirta's (2008) model, the shell height (H_t) as a function of mussel age (t) can be reconstructed with the following equation:

$$H_t = H_{cor} + \sum_{t=A_{cor}+1}^{t=A_{max}} h_t \cdot E_t \quad (1)$$

where H_t is the shell height (mm) at time t (age in years), H_{cor} is the height (mm) of the corroded shell portion along the commissural plane, A_{max} is the maximum observed age (i.e., age at time of death), A_{cor} is the age of the corroded area (i.e., the number of missing increments), h_t is the age-dependent adjustment factor for convexly occurring increment growth (fig. 5b in Helama & Valovirta, 2008), and E_t is the external shell increment (mm, perpendicular to winter lines at the surface of the shell) at age t. H_{cor} was measured in the lab with a microscope from the cross-sections. E_t was estimated with the following equation:

$$E_t = \frac{1}{i_t} \cdot I_t \quad (2)$$

where i_t describes the relationship between the internal and external shell increments as a function of age (fig. 4 in Helama & Valovirta, 2008), and I_t is the internal shell increment (perpendicular to winter lines at the shell cross-section). As recommended by Helama and Valovirta (2008), only individuals of 50 years or older were used in the height-at-age reconstructions to avoid spurious fits, making a total of 98 mussel specimens in the subsequent growth model fitting process. The model-based terminal heights of the mussels were evaluated against the measured shell heights as model verification.

2.4 | Growth models

Five nonlinear growth models, covering both juvenile and adult life stages, were fitted to the reconstructed shell height-at-age data to each individual mussel separately. The first was the von Bertalanffy (1938) growth function, which has primarily been applied in FPM and other bivalve age and growth studies (Haag & Rypel, 2011; Hastie et al., 2000; Miguel et al., 2004). The following 3-parameter von Bertalanffy growth function equation was used:

$$H_t = H_{inf}\left(1 - e^{-k(t-t_0)}\right) \quad (3)$$

where H_t is the shell height (mm) at time t (age in years), H_{inf} is the asymptotic height (mm), k is a growth constant that describes the rate at which H_{inf} is reached (year^{-1}) and t_0 is the theoretical age at which the height of the organism is zero (von Bertalanffy, 1938; Ricker, 1975).

The second was the Lester biphasic growth model, which is considered to perform well for species that mature relatively late and have long reproductive life spans (Lester et al., 2004). The Lester biphasic growth model consists of two separate equations for pre-maturity (all surplus energy invested to somatic growth) and post-maturity (surplus energy invested also to reproduction) periods (Lester et al., 2004). The growth in the pre-maturity period (t < age at maturity [T]) was modelled with a linear model fitted to immature size-at-age data:

$$H_t = h \cdot t + c \tag{4}$$

where h is juvenile growth rate (mm year^{-1}) and c is the intercept of the linear fit to immature growth (mm). T was set to 20 years as it is the expected age at maturity for FPM at our sampling latitudes (Arvidsson et al., 2012; Ziuganov et al., 1994). The x-intercept of the linear model is the hypothetical age at which mussel height is zero, denoted as $t_{H=0}$. We used h, $t_{H=0}$ and T in modelling the growth in the post-maturity period ($t \geq T$) with mature size-at-age data and the following von Bertalanffy growth function, derived from Lester et al. (2004, eqs. 3.2, 3.3 and 3.4):

$$H_t = \left(h/\left(e^k - 1\right)\right) \cdot \left(1 - e^{\left(k \cdot \left(\left(T + \ln\left(1 - \left(e^k - 1\right) \cdot \left(T - t_{H=0}\right)\right)/k\right) - t\right)\right)}\right) \tag{5}$$

where only the parameter k is unknown. The Lester biphasic growth model allows the amount of energy invested in reproduction to be estimated with the following expression from Lester et al. (2004, eq. 3.3):

$$g = 3 \cdot \left(e^k - 1\right) \tag{6}$$

where g is the investment in reproduction (gonad weight/somatic weight). When g is solved, H_{inf} and t_0 can be calculated with the equations from Lester et al. (2004, eqs. 3.2 and 3.4). In rare occasions, the pre-maturation growth could not be observed, and therefore, the Lester biphasic growth model could not be fitted.

The third and fourth models were two sigmoidal growth (S-shaped) models. Both the Gompertz and logistic growth model have three parameters, but the former one is not symmetrical around the inflection point. We used self-starting model functions, which do not require initial values for the model parameter estimates. The Gompertz model was parameterized as follows:

$$H_t = H_{inf} \cdot e^{\left(-bc^t\right)} \tag{7}$$

where b is the displacement of the curve on the x-axis and c is the growth rate. The generalized logistic function was parameterized as follows:

$$H_t = H_{inf} / \left(1 + e^{\left(t_{mid} - t\right)/scal}\right) \tag{8}$$

where t_{mid} is the age when mussels have reached half of the asymptotic height (i.e., the inflection point), and $scal$ is a scaling parameter for the x-axis with which the growth rate can be calculated as $1/scal$.

The fifth model was a power law model where the annual increase in shell height ($\delta H_t = H_{t+1} - H_t$) is equal to the mussel age raised to a power:

$$\delta H_t = at^b \tag{9}$$

where a is the absolute rate of growth and b is the rate at which the asymptotic size is approached. Under logarithmic transformation, the power law relationship become linearized:

$$\log 10(\delta H_t) = \log 10(a) + \mathrm{b} \cdot \log 10(t) \tag{10}$$

In order to estimate a and b in Equation (9), we fitted a log–log linear regression model to the data according to the Equation (10), where b is equivalent to the slope of the linear regression and a is the inverse-log transform of the y-intercept estimate. After solving a and b, the mussel height at certain age can be estimated with the integral of δH_t with the following equation:

$$H_t = H_{start} + \int_{t_{start}}^{t_n} at^b.dt \tag{11}$$

where H_{start} is the height (mm) at the first observed annual increment, t_{start} is the age (years) of the first observed increment, and t_n is any given age (years). H_{inf} was estimated by setting t_n in Equation (11) to infinity (∞).

In addition to the five models used to cover both juvenile and adult life stages, we additionally parameterized a sixth model for juvenile life stage only to test if the individual mussels followed exponential growth in the pre-maturity phase (up to the age of 19 years). We used an exponential growth model of the following form:

$$H_t = ab^t \tag{12}$$

where a is the initial model value H_t when t is zero and b is the growth rate. Exponential growth model can be linearized using the natural logarithm of the response variable:

$$\ln(H_t) = \ln(a) + t \cdot \ln(b) \tag{13}$$

We estimated a and b in Equation (12) with a log-level linear regression model according to the Equation (13), where a and b are the inverse-natural log transform of the y-intercept estimate and the slope of the linear regression model, respectively. After solving a and b, the size at given age can be estimated with the Equation (12).

We did not have height observations between ages 0 to 7 years due to shell erosion. Therefore, the height of the FPM individuals at age 1 ($H_{t=1}$) was set to 0.343 mm ($n = 57$), which is an estimate of average shell height for FPM bred in captivity at the end of their

parasitic life stage (approximately 1 year old) (unpublished data). This approach facilitated the direction of the growth curves to biologically reasonable estimates. The additional data point were used in all models, except the power law model, because the latter require consecutive height observations.

The parameters of all the models were estimated separately for each mussel individual. All the nonlinear models were fitted by nonlinear least-squares regression. The goodness of model fits to the height-at-age data were evaluated by visual inspection of the fitted lines and by comparing model regression coefficients (R^2), sums of squared residuals (RSS) and residual standard errors (RSE). Although the models have different model parameters, we could compare their associated estimates of asymptotic sizes. The models were compared with each other also with the deviances of the model height estimates from the observed shell heights, which were calculated subtracting the observed shell height at age t from the fitted shell height at age t.

Statistical modelling was done using R (v. 4.2.1, R Core Team, 2022), the stats, the FSA (Ogle et al., 2022) and the minpack.lm packages (Elzhov et al., 2023).

3 | RESULTS

3.1 | Maximum shell size and age

The observed A_{max}, L_{max} and H_{max} values for each population are given in Table 1. The maximum life span showed remarkable variation across the populations, as the A_{max} of the populations ranged from only 54 years (River Vuoksioja) to 254 years (River Lovttajohka). Variation can be seen also in the maximum shell sizes. The L_{max} and H_{max} ranged from 83 mm (River Mutajoki) to 140 mm (River Merenoja), and 41 mm (River Mutajoki) to 65 mm (River Lohijoki and River Lutto), respectively. Size, age and H_{cor} of all mussel individuals can be found in the open data publishing platform Dryad (see Data availability statement).

3.2 | Reconstructed shell heights

The measured shell heights indicated that mussels of similar age had different sizes, showing that the growth rate of FPM is highly variable across the study area (Figure 1a). The shell height growth reconstruction model showed reasonable skill in reconstructing the measured heights of the mussels. After accounting for outliers (Figure S2), linear regression showed low but statistically significant and positive relationship between the measured and reconstructed shell heights at the time of death (Figure 1b, adj. $R^2 = 0.401$, F-statistic $= 63.91$, $df = 93$, $p < 0.001$).

The resulting growth trajectories from reconstructed shell heights of individual mussels revealed remarkable variation in size-at-age among the studied populations (Figure 2). For example, at 20 years of age (corresponding maturation; e.g., Ziuganov et al., 1994) the smallest and largest reconstructed heights were in average (± standard deviation) 14.2 mm (±1.0) in River Kivijoki and 39.9 mm (±4.0) in River Ljusträskbäcken, respectively (Figure 2). Variation in growth patterns can be seen also within populations, although is not as prominent as the among-river variation and our sample size per population was relatively small ($n = 1$–6; Table 1 and Figure 2). Visually inspecting, the shapes of the growth trajectories appear to be influenced by the age at time of death so that slower growth rates are associated with higher age at death (Figure S3). In addition, there is indication that only few individuals had reached the phase in their life span where the growth rate began to plateau, meaning that the growth was still significantly incomplete (Figure 2).

3.3 | Growth models' parameters and performance

The growth models were applied to the individual shell growth history reconstructions presented in Figure 2. The von Bertalanffy growth model and logistic growth model converged for all the individuals. However, the Gompertz, Lester biphasic and power law growth models failed to converge 25, 16 and 3 times out of 98 individuals, respectively. There was some within-river variation in the performance of the growth models, but overall, the von Bertalanffy growth model was in average the model with the lowest RSS (113.1) and RSE (1.1), and highest R^2 (98.5%) (Table 2, Figure S4). The von Bertalanffy growth model outperformed the other models for 58.2%–70.4% of the mussel individuals. For comparison, Gompertz and Lester biphasic growth models' relative performance was 21.4%–25.5% and 4.1%–20.4%, respectively. The relative performance of the logistic and power law models was 0%. In addition, the power law model showed in average remarkably high RSS and RSE and low R^2. This was likely caused by the fact that the power law model had one height observation less (i.e., $H_{t=1} = 0.343$ mm) than the other models for each individual during the curve fitting process, but the goodness-of-fit estimators were calculated on the same number of residuals so that all estimators would be comparable.

The visual inspection of the fitted growth curves showed that the von Bertalanffy growth model is generally a good growth model for FPM, but it also revealed that the model tends to underestimate the H_{inf} (asymptotic height) of the mussel individuals (Figures S5 and S6). Nevertheless, Gompertz and logistic growth models systematically estimate even smaller H_{inf} than the von Bertalanffy model. The number of cases where Gompertz growth model was the one fitting the best to a given individual increased slightly towards the southernmost catchments and decreased by age category (Figure S4). A closer look to the Gompertz model fits however reveals that, even if based on the RSS and RSE and R^2 values it outperformed the other models for some mussel individuals, in most of these cases the fitted Gompertz growth curves do not visually seem to fit the reconstructed height-at-age data better than the von Bertalanffy (Figure S5).

The average of the von Bertalanffy growth model parameter estimates are listed in the Table 3. Average growth constant k estimates for the studied rivers ranged from 0.018 year^{-1} (River Hanhioja) to 0.057 year^{-1} (River Mutajoki and River Porontimajoki).

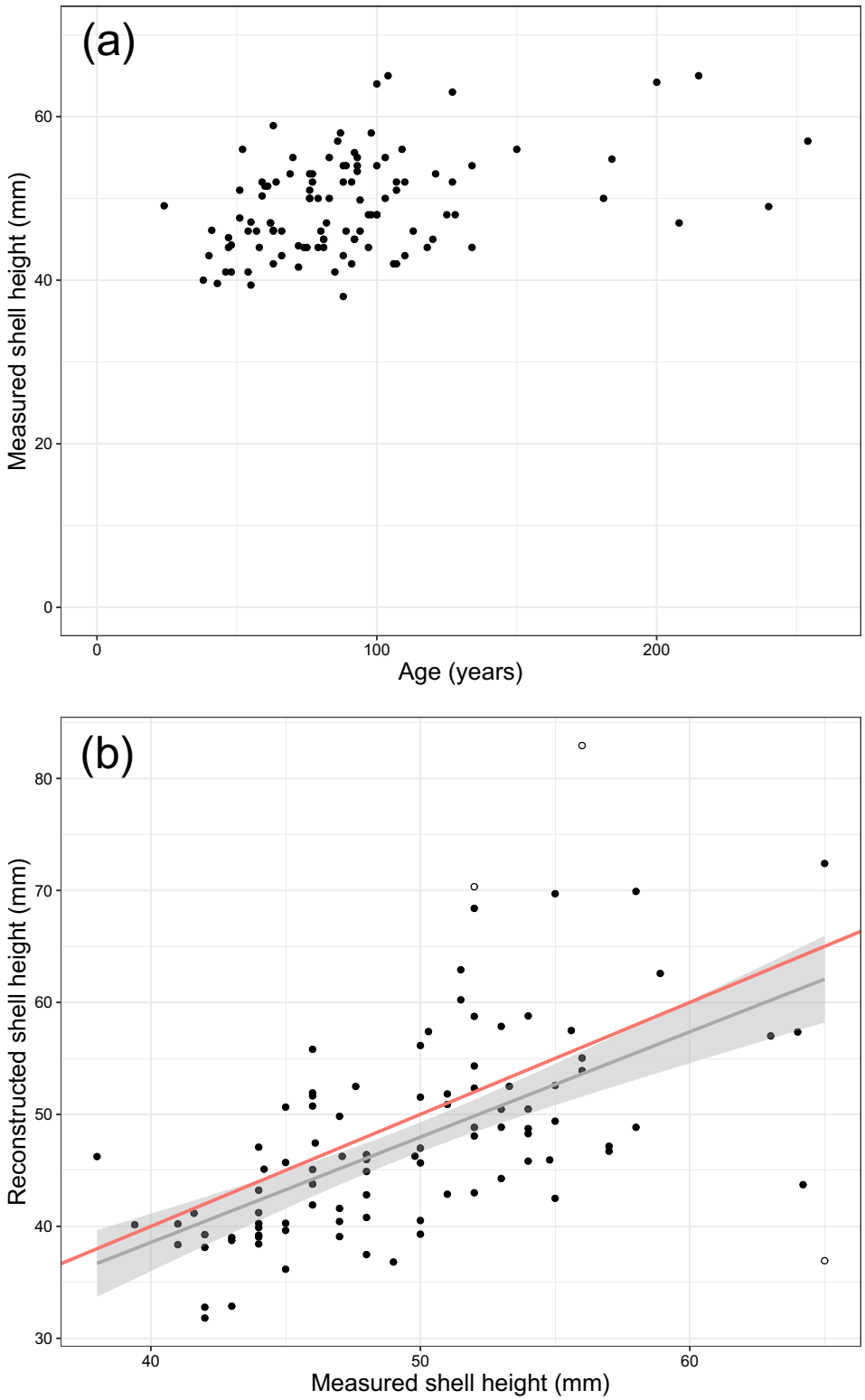

FIGURE 1 (a) Measured shell heights plotted against the age of the freshwater pearl mussel (*Margaritifera margaritifera*) individuals (108 individuals from 34 populations). (b) Linear regression between the reconstructed shell heights and measured shell heights at the time of death (in total 98 individuals of age ≥50 years). *Adj.* $R^2 = 0.401$, *F-statistic* = 63.91, *df* = 93, *RSE* = 6.46, $p < 0.001$. Black dots represent the data points, empty dots the outliers. Grey line is the regression line, and grey area is the 95% confidence region. Red line represents a line with slope of 1.

Average estimates of H_{inf} and t_0 ranged from 37.5 mm (River Saukkojoja) to 79.5 mm (River Lohijoki) and from −6.5 years (River Lovttajohka) to 3.9 years (River Humalajoki), respectively. Data summarizing the average Gompertz, logistic, Lester biphasic, and power law growth model parameters can be found in the open data publishing platform Dryad (see Data availability statement).

3.4 | Deviance of the predicted sizes from the reconstructed sizes

The deviances of the modelled shell heights from the reconstructed shell heights are illustrated in Figure 3a for the adult phase and in Figure 3b for the juvenile phase (see also Figure S7).

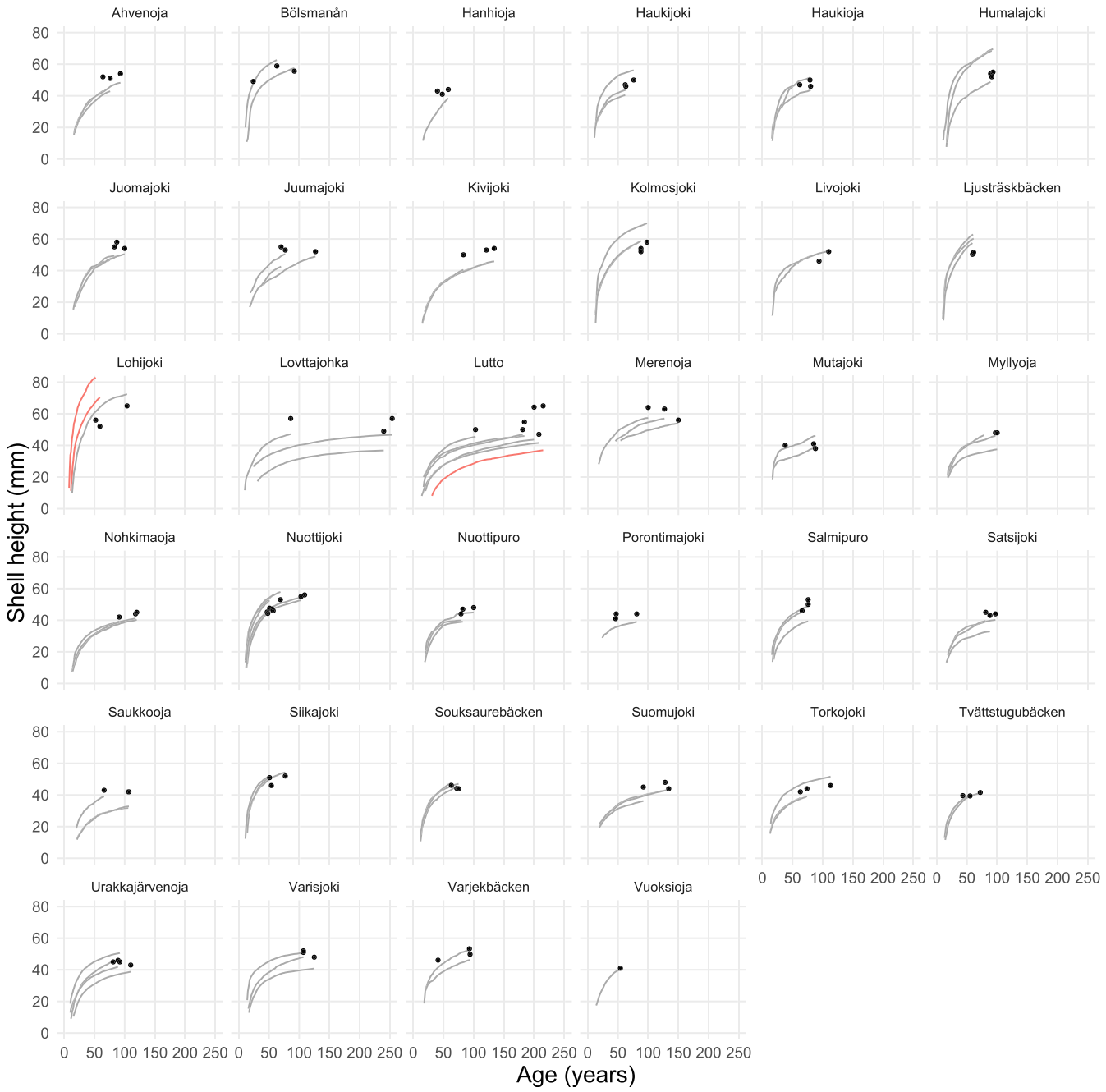

FIGURE 2 Reconstructed shell height-at-age of the freshwater pearl mussel (*Margaritifera margaritifera*) individuals by population (in total 98 individuals of age ≥50 years from 34 populations). Grey lines represent the individuals reconstructed growth history. Red lines represent the outlier individuals (see Figures 1b and S2). Dots indicate the measured heights of the mussels at the time of collection/death.

Overall, most of the deviance in the height in the adult phase falls between −2.5 and 2.5 mm (Figure 3a). From all the models, the von Bertalanffy growth model has lowest deviance from the 0-line (i.e., no difference between the modelled and reconstructed height) and the model's distributions are narrower compared with the other growth models distributions. However, from 180 years age onwards all the models appear to underestimate the reconstructed heights, except for the power law model from approximately 200 years onwards.

Figure 3b shows that in general the fitted juvenile (<20 years old) heights deviate more from the reconstructed heights than the fitted adult heights. However, size-and-age data for ages from 2 to 7 years were not obtained because of shell corrosion, and thus these ages' reconstructed heights could not be compared with the modelled heights. The age specific differences in the predicted and reconstructed heights show that the power law model can fit juvenile heights with the lowest deviance from the reconstructed heights when compared with the other growth models (Figure 3b). However,

TABLE 2 Goodness-of-fit of the growth models evaluated by RSS (sum of squared residuals), RSE (residual standard error), and R^2 (regression coefficient).

	RSS			RSE			R^2		
Model (*n*)	Mean	CI	Rel. perf. (%)	mean	CI	Rel. perf. (%)	mean	CI	Rel. perf. (%)
von Bertalanffy (98)	113.1	87.0–139.1	58.2	1.1	1.0–1.2	70.4	0.985	0.982–0.987	69.4
Gompertz (73)	123.4	97.7–149.0	21.4	1.2	1.1–1.4	25.5	0.984	0.983–0.986	25.5
Logistic (98)	225.5	192.1–258.9	0.0	1.7	1.5–1.8	0.0	0.966	0.962–0.969	0.0
Lester (82)	561.8	307.3–816.2	20.4	3.0	2.5–3.4	4.1	0.851	0.797–0.904	5.1
Power (95)	53,478,531	−50,254,839–157,211,900	0.0	143.0	−49.6–335.7	0.0	−17068	−50372–16237	0.0

Note: Mean indicates the average of all the converged models and CI the confidence interval by model type (*n* of converged models in brackets next to model name). The relative performance of the models equals to the proportion of cases (% out of 98 individuals) in which the model outperformed the other models based on the used goodness-of-fit estimator.

the power law model cannot fit the first year's observation, because it does not have height observations for $H_{t=1}$. When compared with the power law model, the von Bertalanffy, Gompertz, logistic and Lester biphasic growth models tend to have higher variation in the estimated juvenile heights from age 8 to 19 years and to overestimate the reconstructed size before moving towards the 0-line. Overall, the exponential growth model seems to be a poor model in estimating juvenile pearl mussel heights.

4 | DISCUSSION

4.1 | Performance of the growth models

The performance of the von Bertalanffy model in estimating the growth of FPM have been also earlier compared with alternative models. For example, Hastie et al. (2000) found that the von Bertalanffy growth model performed the best when compared with the power law and logistic models. Miguel et al. (2004) instead found that the von Bertalanffy model and hyperbolic function were similar in their performance, but the hyperbolic function appeared to be applicable only from 6 years of age onwards. We investigated the performance of the von Bertalanffy and four other growth models with several performance descriptors (e.g., residuals and descriptive power), which all supported the use of the former (e.g., relative performance always higher than 50%) when modelling the growth of the FPM within our study area. Our results align with previous studies, which have shown von Bertalanffy to reflect FPM and other Unionida growth patterns (e.g., Haag & Rypel, 2011; Hastie et al., 2000; Miguel et al., 2004).

Regardless the better performance of the von Bertalanffy model, previous FPM growth studies have addressed issues in modelling the growth in the youngest age classes (Hastie et al., 2000; Miguel et al., 2004). Therefore, we also compared the performance of six different growth models in estimating juvenile phase growth. From all the fitted models, we found the power law model to yield the most accurate age-dependent height estimates for the juvenile phase as its height estimates had the smallest deviance from the reconstructed heights. This supports the view that a single growth model may not be able to reflect the entire life span of this species (Hastie et al., 2000; Miguel et al., 2004). While the von Bertalanffy can be considered a good general descriptor of growth for the FPM, we propose the power law model to be the most appropriate growth model to estimate juvenile FPM growth when annual shell growth increments can be retrieved for this life stage.

The growth models applied in our study differed also in their ability to reflect the growth in the oldest age classes. The von Bertalanffy, Gompertz and logistic growth models reached the asymptotic phase generally earlier than the final reconstructed heights of the mussels would indicate, meaning that these models systematically underestimated the H_{inf} of the mussel individuals. Miguel et al. (2004) made similar finding with the von Bertalanffy growth model in their study. As recommended by Helama and Valovirta (2008), we aimed at avoiding spurious parametrizations by

TABLE 3 Average von Bertalanffy growth model parameter estimates and confidence intervals (CI) for 34 freshwater pearl mussel populations. The model was fit individually on height-at-age data.

River	Mean H_{inf} (CI)	Mean k (CI)	Mean t_0 (CI)	n of converged models
Ahvenoja	50.01 (46.99–53.04)	0.030 (0.027–0.033)	1.14 (0.30–1.98)	3
Bölsmanån	60.75 (23.29–98.22)	0.052 (−0.046–0.150)	2.64 (−12.25–17.53)	2
Hanhioja	61.58 (NA)	0.018 (NA)	1.53 (NA)	1
Haukijoki	47.88 (28.18–67.59)	0.056 (0.049–0.063)	1.57 (0.65–2.49)	3
Haukioja	55.08 (30.98–79.18)	0.035 (0.013–0.057)	2.43 (−0.05–4.90)	3
Humalajoki	63.97 (36.41–91.52)	0.038 (0.018–0.058)	3.93 (2.19–5.68)	3
Juomajoki	52.77 (48.60–56.93)	0.033 (0.024–0.042)	2.60 (2.18–3.01)	3
Juumajoki	52.89 (50.73–55.05)	0.026 (0.007–0.045)	−0.35 (−5.87–5.16)	3
Kivijoki	46.44 (44.81–48.06)	0.025 (0.025–0.026)	3.46 (−0.70–7.62)	3
Kolmosjoki	63.89 (51.18–76.59)	0.038 (0.025–0.050)	2.06 (0.92–3.20)	3
Livojoki	52.25 (42.31–62.19)	0.037 (−0.027–0.101)	1.00 (−12.16–14.15)	2
Ljusträskbäcken	63.67 (59.26–68.07)	0.049 (0.030–0.068)	2.16 (1.53–2.79)	3
Lohijoki	79.47 (63.88–95.05)	0.047 (0.013–0.081)	3.09 (0.00–6.19)	3
Lovttajohka	43.54 (28.61–58.48)	0.027 (−0.007–0.061)	−6.47 (−31.18–18.24)	3
Lutto	43.29 (39.82–46.75)	0.023 (0.015–0.030)	−1.57 (−6.73–3.59)	6
Merenoja	56.74 (50.14–63.35)	0.031 (0.016–0.046)	0.33 (−0.16–0.83)	3
Mutajoki	40.01 (−12.04–92.05)	0.057 (0.023–0.092)	0.58 (−3.35–4.51)	2
Myllyoja	43.94 (28.84–59.04)	0.041 (0.030–0.052)	1.00 (−0.20–2.19)	3
Nohkimaoja	41.06 (37.48–44.64)	0.032 (0.015–0.049)	2.24 (−1.68–6.15)	3
Nuottijoki	57.61 (53.87–61.35)	0.043 (0.036–0.050)	2.55 (1.91–3.18)	6
Nuottipuro	43.95 (39.50–48.39)	0.039 (0.031–0.048)	2.29 (−0.76–5.34)	3
Porontimajoki	38.71 (NA)	0.057 (NA)	0.78 (NA)	1
Salmipuro	48.43 (38.19–58.66)	0.037 (0.027–0.047)	1.79 (0.61–2.97)	3
Sätsijoki	38.37 (27.77–48.96)	0.040 (0.032–0.048)	1.13 (−0.03–2.29)	3
Saukko-oja	37.51 (24.44–50.58)	0.030 (0.019–0.041)	2.13 (−0.20–4.46)	3
Siikajoki	56.43 (54.85–58.00)	0.050 (0.037–0.064)	1.89 (1.21–2.58)	3
Souksaurebäcken	48.58 (43.03–54.13)	0.046 (0.035–0.058)	2.00 (0.88–3.12)	3
Suomujoki	40.54 (31.65–49.43)	0.034 (0.020–0.047)	−0.79 (−4.67–3.09)	3
Torkojoki	43.36 (27.67–59.05)	0.045 (0.036–0.055)	0.35 (−1.67–2.36)	3
Tvättstugubäcken	44.54 (41.23–47.86)	0.042 (0.003–0.082)	2.16 (−4.56–8.88)	2
Urakkajärvenoja	44.66 (37.12–52.20)	0.041 (0.028–0.054)	1.33 (−0.85–3.51)	4
Varisjoki	46.40 (34.31–58.49)	0.042 (0.013–0.070)	1.30 (−1.63–4.22)	3
Varjekbäcken	49.75 (2.73–96.76)	0.038 (0.024–0.052)	0.23 (−9.63–10.08)	2
Vuoksioja	46.62 (NA)	0.040 (NA)	1.27 (NA)	1

Note: H_{inf} = asymptotic shell height (mm), k = growth rate (year^{-1}), t_0 = theoretical age at which the length of the organism is 0 (years).

fitting the growth models to only ≥50 years old individuals. The reconstructed growth trajectories however suggested that the growth of many of the mussel individuals might have been still significantly incomplete. As the models are dependent on having observations for all the age classes (Haag, 2009; Kritzer et al., 2001; Pardo et al., 2013), the systematic underestimation of the H_{inf} could be caused by fitting the models to data showing incomplete growth characteristics. Because the von Bertalanffy curves in this study underestimate the H_{inf}, extrapolating beyond the range of age observed in the studied populations should be avoided as it can lead to biased size estimates.

4.2 | Plasticity in longevity and growth

Longevity (A_{max}) and growth parameters (k, L_{max}, H_{max} and H_{inf}) show considerable variation in our study area, which is consistent with previous regional studies (e.g., Hastie et al., 2000; Helama & Valovirta, 2008; Miguel et al., 2004; Table S1). Fennoscandian FPM populations show similar L_{max} values and variation in L_{max} (83–140 mm) as previously reported in other European countries (Hastie et al., 2000; Miguel et al., 2004; Ziuganov et al., 2000; Table S1). However, for many of the current populations, L_{max} values observed

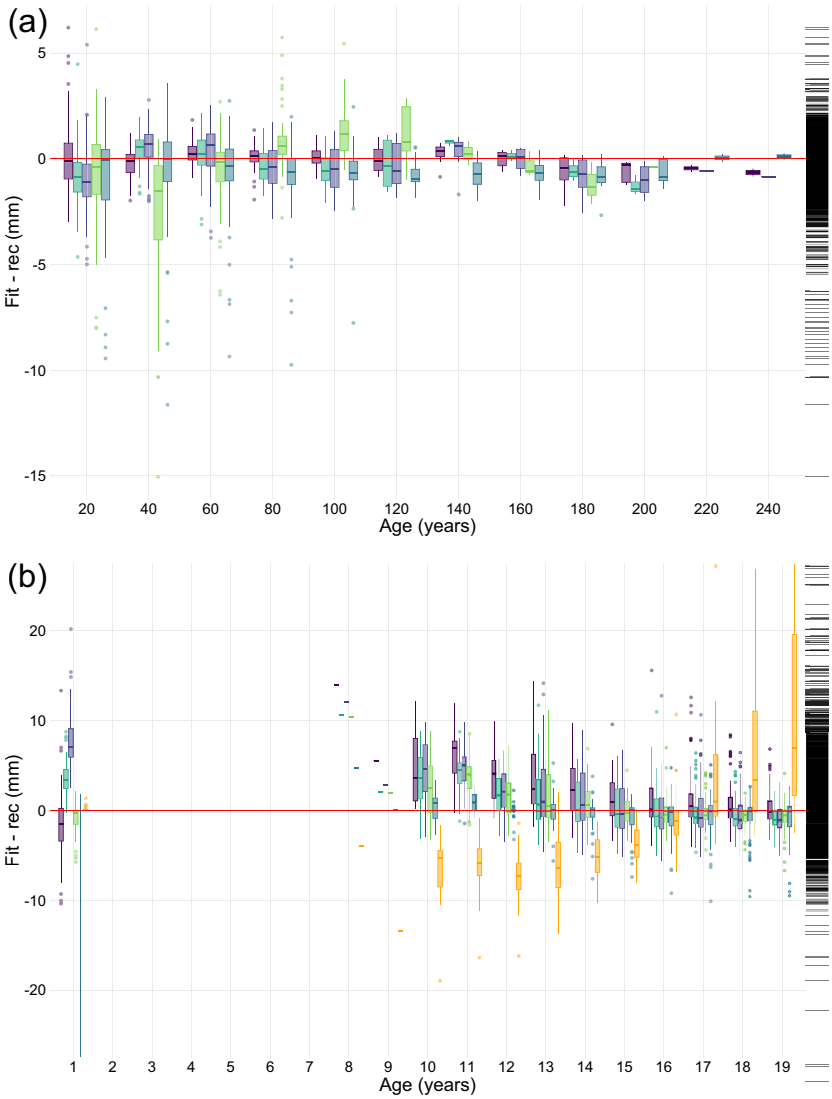

FIGURE 3 Distributions of age specific differences in height predicted by the growth models and the reconstructed height (fit–rec, mm) in (a) adult (ages ≥20 years) and (b) juvenile stage (age between years 1 and 19). The red line indicates 0 mm difference between the fitted value and the reconstructed value. von Bertalanffy = dark purple, Gompertz = light blue, logistic = light purple, Lester biphasic = green, power law = dark blue, exponential = orange. Bold horizontal lines in boxplots correspond to the median. The lower and upper hinges of the boxes indicate the first and third quartiles. The whiskers represent the minimum and maximum values within 1.5 * interquartile range (IQR). Dots indicate outlying points (i.e., < or > than 1.5 * IQR). Density of the data is illustrated in black in the right margin of the plot.

here were lower than those reported elsewhere (Oulasvirta et al., 2015; Oulasvirta et al., 2023; Oulasvirta et al., 2021). This might imply that our samples did not always consist of the largest and oldest individuals, and thus, the true L_{max} and A_{max} for these populations remain unobserved. Nonetheless, our study shows that FPMs in Finland are extremely long lived (A_{max} = 54–254 years), especially when compared with their conspecifics from populations in southern and central Europe (Bauer, 1991; Bauer, 1992; Miguel et al., 2004; Table S1). Some of the mussel individuals studied here were among the oldest recorded of this species, and the A_{max} of 254 years estimated for River Lovttajohka is to our knowledge the oldest reported in Finland. Extremely old specimens have been found also in other northern countries. For example, Dunca et al. (2011) observed several FPM individuals of over 100 years old and one 280 years old in Sweden. However, here the A_{max} ranged from only 61 years to 94 years for the Swedish populations.

Bauer et al. (1991) and Bauer (1992) were the first to study the variation in FPM life-history traits across its distribution area, and to argue FPM's longevity to increase and the growth rate k to decrease towards higher latitudes, as in other ectotherms (e.g., Ricker, 1979). Since then, the latitudinal trend in FPM life-history traits has been discussed by several authors (e.g., Hastie et al., 2000; Helama & Valovirta, 2008; Miguel et al., 2004), and it has been associated with lower water temperatures and shorter growing seasons in northern latitudes (e.g., Dunca & Mutvei, 2001; Schöne et al., 2004). Our and previously published results seem to align with Bauer's findings at larger geographical range (Table S1). However, the temperature regime of the rivers and, thus, the growth and life span of freshwater mussels can vary considerably also within limited geographical areas (e.g., Dunca et al., 2011; Table S1); and within our study area, latitude explains only partly the variation in growth constant k (*adj.* R^2 = 0.22, F-statistic = 10.47, df = 32, p = 0.003) and A_{max} (*adj.* R^2 = 0.14, F-statistic = 6.37, df = 32, p = 0.017). This gives further support to the view that latitude is not the only factor influencing the variation in life-history traits of FPM and underlines the influence of other environmental variables affecting the local conditions, such as the temperature (Dunca et al., 2011) and biological productivity (Bauer et al., 1991; Bauer, 1992; Kesler et al., 2007) — factors which were

not addressed in the present study. In addition, FPM can be adapted to different host fish in different rivers (Atlantic salmon or brown trout; Salonen et al., 2017), which possibly influences the growth but could not be considered in the present study as the fish host status of the present FPM populations is largely unknown.

4.3 | Implications for conservation

Traditionally growth models require large sample sizes so that the size-at-age data could cover the growth trajectories of a population from juvenile to adult (Haag, 2009; Kritzer et al., 2001; Pardo et al., 2013). However, with imperilled species the collection of large sample sizes is not often possible or ethical. In addition, in the case of FPM, frequently the young individuals cannot be found due to high juvenile mortality (e.g., Geist & Auerswald, 2007; Österling et al., 2008; Österling et al., 2010). Thus, to avoid destructive sampling, we used a previously validated model (Helama & Valovirta, 2008) to transform series of existing shell internal annual growth increments into estimates of incremental shell height growth. The model showed reasonable skill in reconstructing FPM growth trajectories in the present study. Helama and Valovirta (2008) obtained similar results when they validated the model with FPM specimens collected from Northern and Southern Finland. Also, Helama et al. (2017) successfully used the model to reconstruct the growth of another imperilled mussel species, *Unio crassus*, in Southern Finland. Even though some individual's reconstructed terminal height deviates from their measured height, which may affect the growth model estimates' accuracy, our results show that for most of the individuals the deviance is within acceptable range. Therefore, based on our and previously published results, we encourage the use of the shell growth reconstruction model in future studies, as it can help in avoiding destructive sampling in populations of endangered freshwater mussel species. Furthermore, the model enables the use of existing museum shell collections and age determination data for similar growth studies presented here. Freshwater mussels (Unionida) are among the most imperilled animals (Lydeard et al., 2004; Aldridge et al., 2022). Study on life-history traits was selected as one of the central research priorities for assessing freshwater mussel conservation status at the species level (Ferreira-Rodríguez et al., 2019). Thus, the present approach could be applied also to other endangered freshwater mussel species to get age-structure information needed for conservation management.

The comparatively high life expectancy of FPM may enable high age structure diversity within populations, and therefore promote population stability and resilience to adverse environmental conditions (Carvalho et al., 2023; Haag & Rypel, 2011; Roff, 1992). FPM's long reproductive life span may represent an example of portfolio effect where the risk of experiencing unfavourable environmental conditions and reproductive failure is spread over time and multiple age classes (Carvalho et al., 2023; Schindler et al., 2010). This may enhance the reproductive output of the population and maintain the population between favourable recruitment events (Berkeley et al., 2004; Carvalho et al., 2023). The risk spreading, however, may not be effective if high juvenile mortality is prolonged over decades — a situation that currently describes most FPM populations (Geist, 2010).

Gaining knowledge on the age structure of target FPM populations is important because the age structure highly influences the growth and recovery potential of populations (Charnov, 1993; Roff, 1992; Stearns, 1992). The von Bertalanffy parameters estimated in the present study can, together with the inverse form of the von Bertalanffy growth equation, be utilized to estimate the age of individuals measured in field or to transform existing shell size distribution datasets to age distributions. These parameters can be used also to estimate the population-specific size at maturation age (we expected it to be 20 years [Arvidsson et al., 2012; Ziuganov et al., 1994]; see Table S2). As the proportion of juvenile mussels in the population is one of the main criteria in judging the viability of FPM in Fennoscandia (Oulasvirta et al., 2017), this information is useful in evaluating population-specific threshold for average size at maturity and to estimate more accurately the proportion of juvenile mussels in the populations. Currently, the viability criteria do not consider population-specific size differences at juvenile age, which are however evident in our and previous growth studies.

Bauer (1991, 1992) has argued that there is a high risk of extinction in FPM populations if the average individual growth constant k in a population is high (i.e., >0.1 year^{-1}), and it is combined with high human induced juvenile mortality rate — a view that has been often applied and cited in FPM growth studies. However, we want to propose the use of another metric with a sound theoretical basis (e.g., Hutchings et al., 2012) and empirical support (Hutchings & Kuparinen, 2017) in evaluating FPM populations' risk of extinction and response to threat mitigation: the natural mortality (M). M can be estimated with three parameters, which were derived with the von Bertalanffy growth equation in the present study: asymptotic size (H_{inf} or L_{inf}), growth coefficient k and an estimate of the size at maturity (Charnov et al., 2013). Populations adapted to higher rates of M can be expected to be at lower risk of extinction and have higher recovery potential than those with lower M, as also their maximum per capita population growth tends to be higher (Hutchings & Kuparinen, 2017).

Because the growth models in the present study were built with the height of the shell as the dependent variable, we suggest that the aforementioned estimations should be more accurate when shell height is used as the size variable instead of length. For this reason, we also recommend the shell height to be always measured in future FPM field studies. However, if needed, regression between the length and height can be used to transform the shell heights into lengths. As an example, in Table S2, we model population specific length–height regression models with shell size measurements for the present 29 Finnish populations.

AUTHOR CONTRIBUTIONS

Sabrina Nykänen: Writing—review and editing; writing—original draft; software; formal analysis; visualization; conceptualization; data curation; funding acquisition; investigation. **Jouni Taskinen:** Writing—review and editing; supervision; funding acquisition; conceptualization. **Mahsa Hajisafarali:** Writing—review and editing; investigation. **Anna Kuparinen:** Writing—review and editing; supervision; funding acquisition; conceptualization.

ACKNOWLEDGEMENTS

The authors would like to thank Sakari Kankaanpää, Jonna Kuha, Patrick Olofsson, Panu Oulasvirta and Aune Veersalu for their help in collecting the mussel samples, and Aliona Elena Meret for her guidance in the age determination. We are grateful to Matthew Cobain for the assistance in coding, to Aliona Elena Meret and Panu Oulasvirta for their valuable comments to this manuscript and to Heikki Erkinaro (SALMUS project's coordinator) for making the field work possible. This project has received funding from the European Research Council (ERC) under the European Union's Horizon 2020 research and innovation programme (grant agreement no 770884; AK), the ENI Kolarctic Cross Border Collaboration (CBC) Programme (SALMUS project, KO1017; JT), the EU LIFE Programme (LIFE Revives project, LIFE20/NAT/FI/000611; JT), the Ellen and Artturi Nyyssönen Foundation (SN), the OLVI Foundation (SN), the Finnish Concordia Fund (SN), the Finnish Foundation for Nature Conservation (SN), and the Biological and Environmental Science Doctoral School of University of Jyväskylä (MH).

CONFLICT OF INTEREST

The authors have no conflict of interest to declare.

DATA AVAILABILITY STATEMENT

Codes and data are available in Dryad (https://doi.org/10.5061/dryad.ncjsxkt2x).

ORCID

Sabrina Nykänen https://orcid.org/0000-0001-6808-8457
Jouni Taskinen https://orcid.org/0000-0003-0098-9560
Mahsa Hajisafarali https://orcid.org/0000-0002-7415-3603
Anna Kuparinen https://orcid.org/0000-0002-7807-8946

REFERENCES

Aldridge, D.C., Ollard, I.S., Bespalaya, Y.V., Bolotov, I.N., Douda, K., Geist, J. et al. (2022). Freshwater mussel conservation: a global horizon scan of emerging threats and opportunities. *Global Change Biology*, 29(3), 575–589. https://doi.org/10.1111/gcb.16510

Arvidsson, B.L., Karlsson, J. & Österling, M.E. (2012). Recruitment of the threatened mussel *Margaritifera margaritifera* in relation to mussel population size, mussel density and host density. *Aquatic Conservation*, 22(4), 526–532. https://doi.org/10.1002/aqc.2240

Atkinson, C.L. & Vaughn, C.C. (2014). Biogeochemical hotspots: temporal and spatial scaling of the impact of freshwater mussels on ecosystem function. *Freshwater Biology*, 60(3), 563–574. https://doi.org/10.1111/fwb.12498

Bauer, G. (1991). Plasticity in life history traits of the freshwater pearl mussel—consequences for the danger of extinction and for conservation measures. In: Seitz, A. & Loeschcke, V. (Eds.) *Species conservation: a population-biological approach*. Birkhäuser: Basel, pp. 103–120.

Bauer, G. (1992). Variation in the life span and size of the freshwater pearl mussel. *The Journal of Animal Ecology*, 61(2), 425–436. https://doi.org/10.2307/5333

Bauer, G., Hochwald, S. & Silkenat, W. (1991). Spatial distribution of freshwater mussels: the role of host fish and metabolic rate. *Freshwater Biology*, 26(3), 377–386. https://doi.org/10.1111/j.1365-2427.1991.tb01405.x

Berkeley, S.A., Hixon, M.A., Larson, R.J. & Love, M.S. (2004). Fisheries sustainability via protection of age structure and spatial distribution of fish populations. *Fisheries*, 29(8), 23–32. https://doi.org/10.1577/1548-8446(2004)29[23:FSVPOA]2.0.CO;2

von Bertalanffy, L. (1938). A quantitative theory of organic growth (inquiries on growth Laws. II). *Human Biology*, 10(2), 181–213.

Carvalho, P.G., Satterthwaite, W.H., O'Farrell, M.R., Speir, C. & Palkovacs, E.P. (2023). Role of maturation and mortality in portfolio effects and climate resilience. *Canadian Journal of Fisheries and Aquatic Sciences*, 80(6), 924–941. https://doi.org/10.1139/cjfas-2022-0171

Charnov, E.L. (1993). *Life history invariants: some explorations of symmetry in evolutionary ecology*. Oxford, New York: Oxford University Press.

Charnov, E.L., Gislason, H. & Pope, J.G. (2013). Evolutionary assembly rules for fish life histories. *Fish and Fisheries*, 14(2), 213–224. https://doi.org/10.1111/j.1467-2979.2012.00467.x

Cuttelod, A., Seddon, M. & Neubert, E. (2011). *European red list of non-marine molluscs*. Publications Office of the European Union.

DuBose, T.P., Atkinson, C.L., Vaughn, C.C. & Golladay, S.W. (2019). Drought-induced, punctuated loss of freshwater mussels alters ecosystem function across temporal scales. *Frontiers in Ecology and Evolution*, 7, 274. https://doi.org/10.3389/fevo.2019.00274

Dunca, E. & Mutvei, H. (2001). Comparison of microgrowth pattern in *Margaritifera margaritifera* shells from north and South Sweden. *American Malacological Bulletin*, 16(1/2), 239–250.

Dunca, E., Söderberg, H. & Norrgrann, O. (2011). Shell growth and age determination in the freshwater pearl mussel *Margaritifera margaritifera* in Sweden: natural versus limed streams. *Ferrantia*, 64, 11.

Elzhov, T.V., Mullen, K.M., Spiess, A.-N. & Bolker, B. (2023). minpack.lm: R interface to the Levenberg–Marquardt nonlinear least-squares algorithm found in MINPACK, plus support for bounds.

Ferreira-Rodríguez, N., Akiyama, Y.B., Aksenova, O.V., Araujo, R., Christopher Barnhart, M., Bespalaya, Y.V. et al. (2019). Research priorities for freshwater mussel conservation assessment. *Biological Conservation*, 231, 77–87. https://doi.org/10.1016/j.biocon.2019.01.002

Gamito, S. (1998). Growth models and their use in ecological modelling: an application to a fish population. *ECOMOD*, 113(1), 83–94. https://doi.org/10.1016/S0304-3800(98)00136-7

Geist, J. (2010). Strategies for the conservation of endangered freshwater pearl mussels (*Margaritifera margaritifera* L.): a synthesis of conservation genetics and ecology. *Hydrobiologia*, 644(1), 69–88. https://doi.org/10.1007/s10750-010-0190-2

Geist, J. & Auerswald, K. (2007). Physicochemical stream bed characteristics and recruitment of the freshwater pearl mussel (*Margaritifera margaritifera*). *Freshwater Biology*, 52(12), 2299–2316. https://doi.org/10.1111/j.1365-2427.2007.01812.x

Geist, J., Thielen, F., Lavictoire, L., Hoess, R., Altmueller, R., Baudrimont, M. et al. (2023). Captive breeding of European freshwater mussels as a conservation tool: a review. *Aquatic Conservation*, 33(11), 1321–1359. https://doi.org/10.1002/aqc.4018

Haag, W.R. (2009). Extreme longevity in freshwater mussels revisited: sources of bias in age estimates derived from mark–recapture

experiments. *Freshwater Biology*, 54(7), 1474–1486. https://doi.org/10.1111/j.1365-2427.2009.02197.x

Haag, W.R. (2013). The role of fecundity and reproductive effort in defining life-history strategies of North American freshwater mussels. *Biological Reviews*, 88(3), 745–766. https://doi.org/10.1111/brv.12028

Haag, W.R. & Rypel, A.L. (2011). Growth and longevity in freshwater mussels: evolutionary and conservation implications. *Biological Reviews*, 86(1), 225–247. https://doi.org/10.1111/j.1469-185X.2010.00146.x

Hastie, L.C., Young, M.R. & Boon, P.J. (2000). Growth characteristics of freshwater pearl mussels, *Margaritifera margaritifera* (L.). *Freshwater Biology*, 43(2), 243–256. https://doi.org/10.1046/j.1365-2427.2000.00544.x

Helama, S. & Valovirta, I. (2008). Ontogenetic morphometrics of individual freshwater pearl mussels (*Margaritifera margaritifera* (L.)) reconstructed from geometric conchology and trigonometric sclerochronology. *Hydrobiologia*, 610(1), 43–53. https://doi.org/10.1007/s10750-008-9421-1

Helama, S., Valovirta, I. & Nielsen, J. (2017). Growth characteristics of the endangered thick-shelled river mussel (*Unio crassus*) near the northern limit of its natural range. *Aquatic Conservation*, 27(2), 476–491. https://doi.org/10.1002/aqc.2698

Howard, J.K. & Cuffey, K.M. (2006). The functional role of native freshwater mussels in the fluvial benthic environment. *Freshwater Biology*, 51(3), 460–474. https://doi.org/10.1111/j.1365-2427.2005.01507.x

Hutchings, J.A. & Kuparinen, A. (2017). Empirical links between natural mortality and recovery in marine fishes. *Proceedings of the Royal Society of London - Series B: Biological Sciences*, 284(1856), 20170693. https://doi.org/10.1098/rspb.2017.0693

Hutchings, J.A., Myers, R.A., García, V.B., Lucifora, L.O. & Kuparinen, A. (2012). Life-history correlates of extinction risk and recovery potential. *Ecological Applications*, 22(4), 1061–1067. https://doi.org/10.1890/11-1313.1

Jokela, J. & Mutikainen, P. (1995). Phenotypic plasticity and priority rules for energy allocation in a freshwater clam: a field experiment. *Oecologia*, 104(1), 122–132. https://doi.org/10.1007/BF00365570

Kesler, D.H., Newton, T.J. & Green, L. (2007). Long-term monitoring of growth in the Eastern Elliptio, *Elliptio complanata* (Bivalvia: Unionidae), in Rhode Island: a transplant experiment. *Journal of the North American Benthological Society*, 26(1), 123–133. https://doi.org/10.1899/0887-3593(2007)26[123:LMOGIT]2.0.CO;2

Kritzer, J.P., Davies, C.R. & Mapstone, B.D. (2001). Characterizing fish populations: effects of sample size and population structure on the precision of demographic parameter estimates. *Canadian Journal of Fisheries and Aquatic Sciences*, 58(8), 1557–1568. https://doi.org/10.1139/f01-098

Lester, N.P., Shuter, B.J. & Abrams, P.A. (2004). Interpreting the von Bertalanffy model of somatic growth in fishes: the cost of reproduction. *Proceedings of the Royal Society of London - Series B: Biological Sciences*, 271(1548), 1625–1631. https://doi.org/10.1098/rspb.2004.2778

Lopes-Lima, M., Sousa, R., Geist, J., Aldridge, D.C., Araujo, R., Bergengren, J. et al. (2017). Conservation status of freshwater mussels in Europe: state of the art and future challenges. *Biological Reviews*, 92(1), 572–607. https://doi.org/10.1111/brv.12244

Lydeard, C., Cowie, R.H., Ponder, W.F., Bogan, A.E., Bouchet, P., Clark, S.A. et al. (2004). The global decline of nonmarine mollusks. *Bioscience*, 54(4), 321–330. https://doi.org/10.1641/0006-3568(2004)054[0321:TGDONM]2.0.CO;2

Miguel, E.S., Monserrat, S., Fernández, C., Amaro, R., Hermida, M., Ondina, P. et al. (2004). Growth models and longevity of freshwater pearl mussels (*Margaritifera margaritifera*) in Spain. *Canadian Journal of Zoology*, 82(8), 1370–1379. https://doi.org/10.1139/z04-113

Ogle, D.H., Doll, J.C., Wheeler, P. & Dinno, A. (2022). FSA: fisheries stock analysis.

Österling, M.E., Arvidsson, B.L. & Greenberg, L.A. (2010). Habitat degradation and the decline of the threatened mussel *Margaritifera margaritifera*: influence of turbidity and sedimentation on the mussel and its host. *Journal of Applied Ecology*, 47(4), 759–768. https://doi.org/10.1111/j.1365-2664.2010.01827.x

Österling, M.E., Greenberg, L.A. & Arvidsson, B.L. (2008). Relationship of biotic and abiotic factors to recruitment patterns in *Margaritifera margaritifera*. *Biological Conservation*, 141(5), 1365–1370. https://doi.org/10.1016/j.biocon.2008.03.004

Oulasvirta, P., Aspholm, P.E., Kangas, M., Larsen, B.M., Luhta, P.-L., Moilanen, E., et al. (2015). Raakku!—freshwater pearl mussel in northern Fennoscandia. Metsähallitus.

Oulasvirta, P., Leinikki, J. & Syväranta, J. (2017). Freshwater pearl mussel in Finland—current status and future prospects. *The Biological Bulletin*, 44(1), 81–91. https://doi.org/10.1134/S1062359017010101

Oulasvirta, P., Olofsson, P., Aspholm, P.E. & Veersalu, A. (2023). *Status of the freshwater pearl mussel populations. Saving our northern freshwater pearl mussel populations*, Vantaa: Metsähallitus, pp. 81–219.

Oulasvirta, P., Saarman, M. & Syväranta, J. (2021). Jokihelmisimpukkapopulaatioiden tilan selvitykset Iijoen vesistöalueella 2021. Alleco Ltd. Report number: 33/2021.

Pardo, S.A., Cooper, A.B. & Dulvy, N.K. (2013). Avoiding fishy growth curves. *Methods in Ecology and Evolution*, 4(4), 353–360. https://doi.org/10.1111/2041-210x.12020

R Core Team. (2022). R: A language and environment for statistical computing.

Régnier, C., Fontaine, B. & Bouchet, P. (2009). Not knowing, not recording, not listing: numerous unnoticed mollusk extinctions. *Biological Conservation*, 23(5), 1214–1221. https://doi.org/10.1111/j.1523-1739.2009.01245.x

Ricker, W.E. (1975). *Computation and interpretation of biological statistics of fish populations*. Ottawa: Department of the Environment, Fisheries and Marine Service.

Ricker, W.E. (1979). Growth rates and models. In: Hoar, W.S., Randall, D.J. & Brett, J.R. (Eds.) *Fish physiology, VIII: bioenergetics and growth*. New York: Academic Press, pp. 677–743.

Roff, D. (1992). *The evolution of life history: theory and analysis*. New York: Chapman & Hall.

Salonen, J.K., Luhta, P.-L., Moilanen, E., Oulasvirta, P., Turunen, J. & Taskinen, J. (2017). Atlantic salmon (*Salmo salar*) and brown trout (*Salmo trutta*) differ in their suitability as hosts for the endangered freshwater pearl mussel (*Margaritifera margaritifera*) in northern Fennoscandian rivers. *Freshwater Biology*, 62(8), 1346–1358. https://doi.org/10.1111/fwb.12947

Schindler, D.E., Hilborn, R., Chasco, B., Boatright, C.P., Quinn, T.P., Rogers, L.A. et al. (2010). Population diversity and the portfolio effect in an exploited species. *Nature*, 465(7298), 609–612. https://doi.org/10.1038/nature09060

Schöne, B.R., Dunca, E., Fiebig, J. & Pfeiffer, M. (2005). Mutvei's solution: an ideal agent for resolving microgrowth structures of biogenic carbonates. *Palaeogeography Palaeoclimatology Palaeoecology*, 228(1), 149–166. https://doi.org/10.1016/j.palaeo.2005.03.054

Schöne, B. R., Dunca, E., Mutvei, H., & Norlund, U. (2004). A 217-year record of summer air temperature reconstructed from freshwater pearl mussels (M. margarifitera, Sweden). *Quaternary Science Reviews*, 23(16–17), 1803–1816. https://doi.org/10.1016/j.quascirev.2004.02.017

Stearns, S.C. (1992). *The evolution of life histories*. Oxford: Oxford University Press.

Strayer, D.L. (2014). Understanding how nutrient cycles and freshwater mussels (Unionoida) affect one another. *Hydrobiologia*, 735(1), 277–292. https://doi.org/10.1007/s10750-013-1461-5

Strayer, D.L., Downing, J.A., Haag, W.R., King, T.L., Layzer, J.B., Newton, T.J. et al. (2004). Changing perspectives on pearly mussels, North America's most imperiled animals. *Bioscience*, 54(5), 429–439. https://doi.org/10.1641/0006-3568(2004)054[0429:CPOPMN]2.0.CO;2

Vaughn, C.C. (2018). Ecosystem services provided by freshwater mussels. *Hydrobiologia*, 810(1), 15–27. https://doi.org/10.1007/s10750-017-3139-x

Vaughn, C.C. & Hakenkamp, C.C. (2001). The functional role of burrowing bivalves in freshwater ecosystems. *Freshwater Biology*, 46(11), 1431–1446. https://doi.org/10.1046/j.1365-2427.2001.00771.x

Young, M.R., Cosgrove, P.J. & Hastie, L.C. (2001). The extent of, and causes for, the decline of a highly threatened naiad: *Margaritifera margaritifera*. In: Bauer, G. & Wächtler, K. (Eds.) *Ecology and evolution of the freshwater mussels Unionoida*. Berlin, Heidelberg: Springer, pp. 337–357.

Ziuganov, V., Zotin, A., Nezlin, L. & Tretiakov, V. (1994). *The freshwater pearl mussels and their relationships with salmonid fish*. Moscow: VNIRO Publishing House.

Ziuganov, V., Miguel, E. S., Neves, R. J., Longa, A., Fernández, C., Amaro, R., Beletsky, V., Popkovitch, E., Kaliuzhin, S., & Johnson, T. (2000). Life span variation of the freshwater pearl shell: A model species for testing longevity mechanisms in animals. *AMBIO: A Journal of the Human Environment*, 29(2), 102–105. https://doi.org/10.1579/0044-7447-29.2.102

SUPPORTING INFORMATION

Additional supporting information can be found online in the Supporting Information section at the end of this article.

How to cite this article: Nykänen, S., Taskinen, J., Hajisafarali, M. & Kuparinen, A. (2024). Growth and longevity of the endangered freshwater pearl mussel (*Margaritifera margaritifera*): Implications for conservation and management. *Aquatic Conservation: Marine and Freshwater Ecosystems*, 34(6), e4205. https://doi.org/10.1002/aqc.4205